Annotation:

Miklip-Module B is a joint project continuing the previous Miklip-I projects Multiclip (764), ALARM (769), MODINI (870)

Project: **764**

Project title: **MULTICLIP**

Project lead: **Johann Jungclaus**

Report period: **1.1.2014 - 31.12.2015**

The target of MiKlip is to develop a model system that is optimized for climate predictions on decadal time scales. Within the MiKlip project, the objective of MULTICLIP is to attain a better understanding of the physical processes in the climate system that are particularly relevant on these time scales and, based on this, to improve their representation in the forecast system. This includes the investigation of the role of ocean-atmosphere coupling in certain regions and the identification of the teleconnection pathways that communicate these signals in the atmosphere.

The focus of our work within the report period was on the role of teleconnections arising from the Atlantic Multidecadal Oscilation (AMO), which describes the leading mode of decadal SST variability in the North Atlantic sector. Motivated by the results from recent studies, which show an impact of the SST in the tropical Atlantic on the tropical Pacific on multi-annual time scales (the so-called "atmospheric bridge"), we have contributed to improved understanding of the interplay between the Atlantic Multidecadal Oscillation and ENSO towards multidecadal to centennial time scales. In particular, the following work was done, using the HLRE II system:

Robustness of AMO-driven ENSO variability over multicentennial timescales (Zanchettin et al., 2015)

We developed a pattern nudging scheme for MPIOM as extension of the original nudging scheme (Zanchettin et al., 2015). In the new implementation, a factor is introduced in the nudging term, that provides spatially-varying and temporally-varying weights to the damping time parameter.

As the first application of this extended nudging scheme, we performed a set of sensitivity experiments conducted with MPI-ESM to assess whether the AMO-ENSO relationship is robust over multicentennial timescales and determine whether atmospheric bridges are sufficient to fully explain AMO-ENSO coupled dynamics. The weighting factor in the new implementation allows to apply a stronger nudging where the signature of the AMO on SSTs is stronger while regions less (or not) affected by the AMO like the North Atlantic storm track region remain free to fully evolve physically consistent.

Three simulations are conducted, in which the SST was nudged towards an AMO-pattern with an idealized sinusoidal temporal evolution. Each of the runs is covering six successive 70-year long oscillations and all initiated from the same restart files. The three simulations differ for the amplitude of the imposed oscillations: amo0.5k describes AMO oscillations with maximum amplitudes of about 0.5 K, which is comparable to the amplitude of AMO fluctuations observed in the 20th century and to the strongest fluctuations spontaneously, but sporadically, generated by MPI-ESM-P (as seen in ctrl); amo1k describes AMO oscillations with amplitudes of about 1 K, i.e., roughly twice the amplitude of observed AMO fluctuations; amo2k describes AMO oscillations with amplitudes of about 2 K, i.e., roughly four-times the amplitude of observed AMO fluctuations.

Our simulations show an AMO-driven modulation of ENSO variance consistent with observations, with AMO inversely correlated with the variance of the Oceanic Niño Index (ONI) (Figure 1a,b). Our interpretation of such behavior follows the "atmospheric bridge-thermocline feedback". In brief, anomalously strong trade winds across the central and western equatorial Pacific and associated thermocline deepening in the Pacific warm pool region during the warm AMO phase weaken the coupled instability through which El Niño events grow, hence reducing ENSO variance.

Our simulations also show an out-of-phase response of ENSO to the AMO, with SST anomalies over the central Pacific becoming warmest during the decades four and five of the AMO oscillation (as shown by persistent positive ONI values, Figure 1c). The residuals of a least-squares linear regression of ONI on the AMO index enhance this out-of-phase behavior of ENSO, which is then linearly independent from the direct thermocline feedback. The mechanism leading to such prolonged period of positive ONI values encompassing the years 35-55 of the AMO are currently under investigation.

Preliminary results suggest that a major role can be ascribed to the upwelling of warm sub-thermocline waters accumulated in the western Pacific warm pool during the warm AMO phase, which is induced by salt-controlled stabilization/destabilization of oceanic stratification. Salinity anomalies in the western Pacific warm pool are therefore imputed to be a major active factor of remotely-driven multidecadal variations in ENSO characteristics and an element of asymmetry for AMO influences on equatorial Pacific climate.

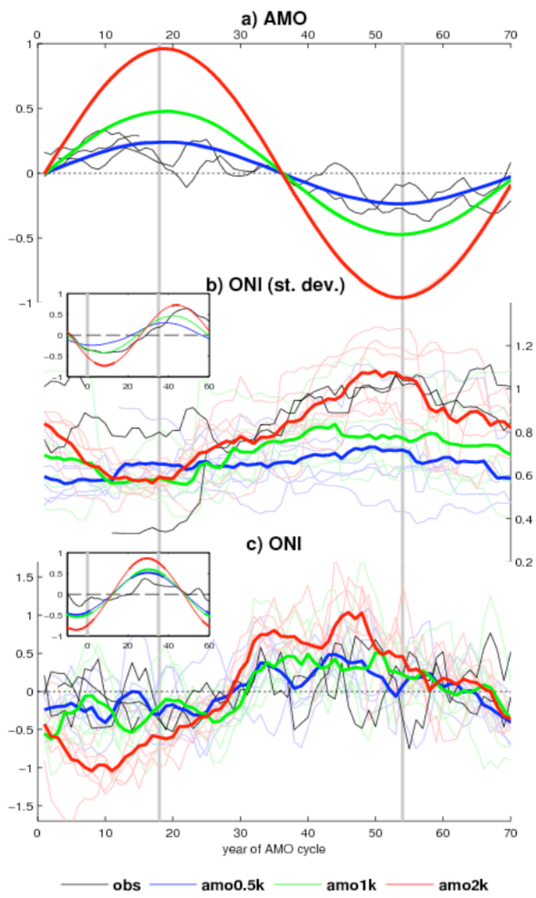

Figure 764. 1: Main panels: evolution of AMO index (a), standard deviation of ONI index over sequential 20-year periods (b) and ONI index (c) during AMO oscillations in observations (black) and AMO simulations (colors, thin lines: individual cycles, thick lines: average cycle). Insets in panels b and c are cross-correlations with the AMO index; statistically significant values are marked with a circle. In all panels, the grey vertical lines mark the approximate maxima of the warm and of the cold phase of the AMO. Data were smoothed with a 5-year running mean low-pass filter.

Publication:

Zanchettin, D., et al., 2015. Mechanisms of out-of-phase response of El Niño to Atlantic multidecadal variability in MPI-ESM. Under review: *Geophysical Reserach Letters.*

Project: **769**

Project title: **Alert for LARge volcanic eruptions in Medium term climate prediction (ALARM)**

Project lead: **Claudia Timmreck**

Report period: **1.1.2014 - 31.12.2015**

The central goal of the MiKlip ALARM project is to study the response of the climate system to volcanic aerosol perturbations and the effects of past historic volcanic eruptions. The allocated resources for the corresponding HLRE project 769 were essential for the following results in the reporting period (Status October 2015):

1. 1 The impact of stratospheric volcanic aerosol on decadal scale predictability

To understand the impact of volcanic aerosol on multi-year seasonal and decadal predictability we performed hindcast simulations over the CMIP5 hindcast period without volcanic aerosol (b1-NVA) using the German MiKlip prediction system and compared them to the corresponding simulations including aerosols (b1-LR) (Timmreck et al., in revision). Our results show that volcanic aerosol significantly affects decadal predictability of global mean surface air temperature in the first years after strong volcanic eruptions (Figure 1). On the regional scale a volcanic imprint on decadal scale variability is visible. Neglecting volcanic aerosol leads to a reduced prediction skill over the tropical and subtropical Atlantic, Indic and West Pacific but to an improvement over the tropical Pacific, where the b1-LR model has no skill. Multi-seasonal differences between both simulations are evident over continental Europe with significant loss of skill due to neglection of volcanic aerosol in boreal winter over central Europe, Scandinavia and over south-eastern Europe and the East-Mediterranean in boreal summer.

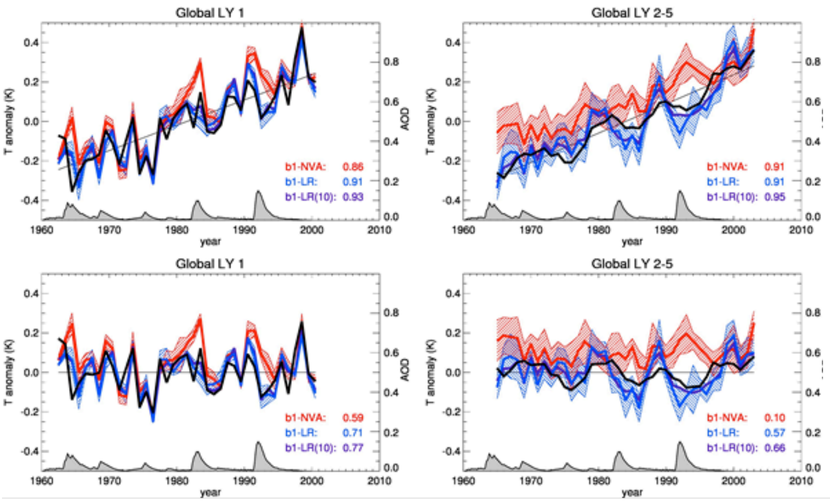

Figure 1 Time series of hindcast and observed anomalies of globally averaged 2m temperature with respect to the mean of 1962-2000 for HadCRUT3v observations [Brohan et al., 2006] (black), b1-LR (blue) and b1-NVA (red). The dashed purple line indicates the 10 member ens. mean of b1-LR. The standard deviation is indicated by the dashed areas. Left panels show the 1st lead year (LY1), right panels the mean of lead years 2-5 (LY2-5). Detrended timeseries are shown at the bottom. The numbers indicate the anomaly correlation coefficient between the hindcasts and observations over the whole period. The grey shaded region shows annual averaged stratospheric aerosol optical depth (AOD) [Stenchikov et al., 1998; and updates].

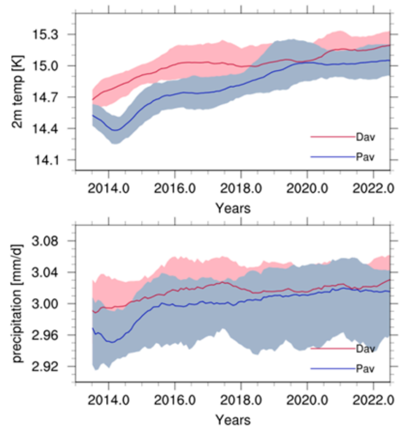

Figure 2: B1-MR simulations for a Pinatubo-like volcanic eruption in 2013. a) Global mean values of 2m temperature and precipitation. The thick line represents the ensemble mean (5 realizations), shaded regions the corresponding min and max range, blue denotes the volcanic cases, red the nonvolcanic ones.

1.2 Impact of future volcanic eruption

We have carried out additional b1(-LR/-MR) simulations with the volcano module to assess the impact of a possible Pinatubo-like volcanic eruption in 2013 and 2015 (Timmreck et al. in prep). Global mean surface temperature and precipitation are reduced for six years but while the predicted global mean near-surface temperature is below the unperturbed ensemble minimum, the precipitation anomalies are within natural variability of the unperturbed run (Figure 2). A clear signal is found in particular in the first two Northern Hemisphere (NH) post eruption winters. The temperature anomaly pattern is similar to reconstructed/observed patterns after large historic eruptions with a warming over Scandinavia and northern Eurasia and a cooling over Greenland and the Mediterranean. In the stratosphere the volcanic signal leads to a phase shift of the Quasi Biennial Oscillation in the b1-MR simulations.

1. 3 Importance of the geographical location and season of the volcanic eruption

To assess the potential radiative impacts of extratropical eruptions compared to tropical eruptions, we have performed MAECHAM5-HAM simulations of eruptions at latitudes spanning the southern tropics (4°S) to the NH high latitudes (64°N). In order to isolate the impact of latitude, eruption characteristics other than latitude, including SO_2 injection magnitude and injection height, are held fixed through the ensemble to values consistent with the 1991 eruption of Pinatubo (Toohey et al., in prep). In contrast to expectations, we find that for Pinatubo-like eruption magnitude and SO_2 injection height, extratropical eruptions can have quite similar global mean radiative impacts as tropical eruptions. In fact, in the NH mean, extratropical eruptions can produce a stronger radiative anomaly than tropical eruptions (Figure 3). The simulation results also show a strong dependence on the season of eruption, with largest NH-mean radiative impact simulated for high latitude eruptions in NH winter (Jan, Figure 3).

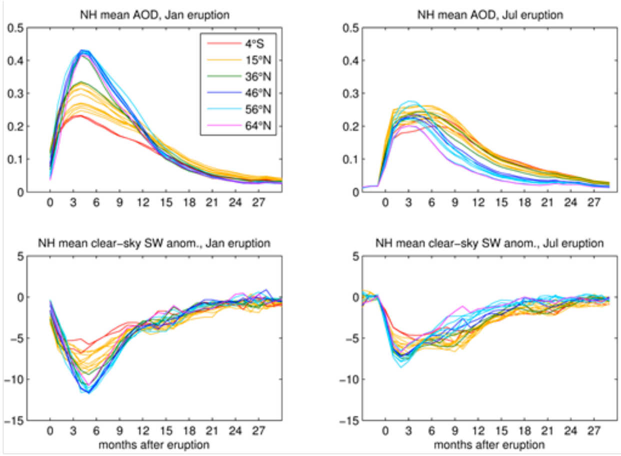

Figure 3: ECHAM5-HAM simulations of the radiative impacts of Pinatubo-like eruptions for varying eruption latitudes. (top) Northern Hemisphere mean aerosol optical depth (AOD) for eruptions in (left) January and (right) July and eruption latitudes as labeled. (bottom) Surface clear-sky short-wave (SW) anomalies.

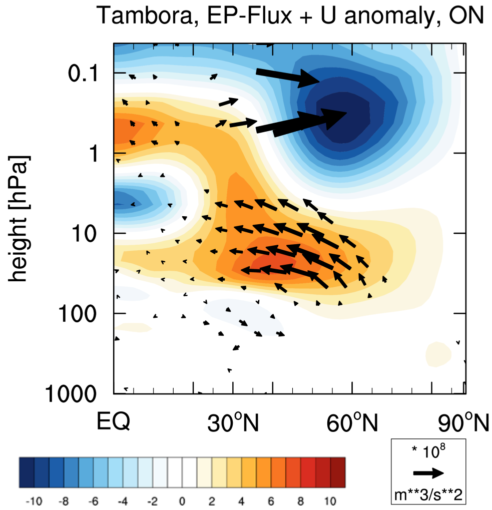

Figure 4: Shaded regions display the ensemble average zonal mean zonal wind anomalies [m/s] averaged over October November in the 1st winter after the Tambora eruption. Arrows show the ensemble average EP-Flux [m^3/s^2]. Only vectors which are significant at the 95% confidence level are shown.

1. 4 Dynamical NH winter response to volcanic eruptions

We have performed additional historical-LR sensitivity runs to assess the influence of the spatial pattern and strength of the volcanic forcing on NH winter climate (Toohey et al., 2014: Bittner et al., to be submitted). Toohey et al. tested the simulated stratospheric dynamical response in the 1st NH winter to 4 different Pinatubo volcanic forcing data sets and found that quite accurate aerosol forcing fields would be necessary to improve predictions of the postvolcanic dynamical response. Bittner et al. found that for a strong enough volcanic forcing (e.g. of Tambora size), the model can reproduce qualitatively the observed stratospheric response in the NH. In contrast to the traditional assumption of a direct impact of the increased stratospheric meridional temperature gradient on the NH polar vortex via the thermal wind balance, significant changes in the vertical wave propagation strengthen the polar vortex. The meridional temperature gradient changes most at 30°N, leading to a positive zonal wind anomaly and subsequent deflection of planetary waves to low latitudes, especially in early winter (Figure 4). These waves will deposit less momentum in the polar stratosphere, which will strengthen the polar vortex.

References[1]

Bittner, M. et al., Sensitivity of the Northern Hemisphere winter stratosphere to the strength of volcanic eruptions. to be submitted to JGR Atmospheres

Brohan , P., et al., Uncertainty estimates in regional and global observed temperature changes: A new data set from 1850, JGR, 111, D12106, doi:10.1029/2005JD006548, 2006

Stenchikov, G. L.,et al, Radiative forcing from the 1991 Mount Pinatubo volcanic eruption, JGR., 103, 13,837–13,858, doi:10.1029/98JD00693, 1998

Timmreck C., et al., The impact of stratospheric volcanic aerosol on decadal scale predictability, in revision for GRL

Timmreck, C. et al., Climate impact of a possible future Pinatubo style eruption, in prep.

Toohey, M., et al., The impact of volcanic aerosol on the Northern Hemisphere stratospheric polar vortex: mechanisms and sensitivity to forcing structure, Atmos. Chem. Phys., 14, 1–16, doi:10.5194/acp-14-1-2014, 2014.

Toohey, M., et al., Revisiting the potential radiative and climatic impact of extratropical vs. tropical volcanic eruptions, in prep for ACP.

[1] ALARM publications are in italic

Project: **870**

Project title: **Modini (MODel INItialisation by partially coupled spin-up)**

Project lead: **Rüdiger Gerdes and Richard Greatbatch**

Report period: **1.1.2014 - 31.12.2015**

The idea behind MODINI (MODel INItialization by partially coupled spin-up) is to create an initialization run by replacing the wind stress seen by the ocean component of a coupled climate model by the time series of the observed wind stress (anomalies), and then to use the resulting model state to launch seasonal and decadal forecasts that are carried out using the free running coupled model. Using the computing resources from this project, MODINI has been applied with some success to the MPI-ESM in the low resolution version (Thoma et al., 2015a, 2015b). A necessary prerequisite is that these initialization runs reproduce the variability of the observed climate system. We have shown that the initialization runs can reproduce ENSO events, the Pacific Decadal Oscillation, the Southern Annular Mode and the interannual variability of the Atlantic Meridional Overturning Circulation (Thoma et al., 2015a). The success of MODINI rests on its ability to reproduce ENSO and the associated teleconnection patterns. This means that the initialization runs not only have skill in the ocean, but also in the atmosphere (e.g. the Aleutian low) despite the fact that the only information about observations that is given to the model is the time series of observed wind stress that is used to drive the ocean component of the coupled model.

We have also shown that MODINI has skill as an initialization for historical forecasts (i.e. hindcasts). Recent results obtained using the MPI-ESM indicate that hindcasts initialized by MODINI on January 1 of each year from 1990 to the 2006 have skill similar to that of the Baseline1 and Prototype MiKlip prediction systems over much of the globe over a wide range of lead times, with better performance over the Pacific sector, including skill in the Pacific sector for years 2-5 and 6-9 for which the Baseline0, Baseline1 and Prototype systems exhibit no skill (Thoma et al., 2015b). Thoma et al. (2015b) also show some skill at hindcasting the global warming hiatus when the MPI-ESM is initialized by MODINI, something the standard MiKlip system is not able to do (see Figure 1 and note the slower rate of warming in the MODINI initialized runs, consistent with observations). Thoma et al. (2015b) also describe a forecast initialized on January 1, 2015 and run out to the end of 2014. This forecast predicts the 2015 El Nino, a switch in the phase of the Pacific Decadal Oscillation and an end to the current global warming hiatus.

MODINI has been applied to the MPI-ESM in different versions. The initialization runs described in Thoma et al. (2015a) used 10 m wind as input and computes wind stress interactively with the ocean state. Here 15 ensemble members were run using NCEP 10 m wind and 10 ensemble members were run using ERA-Interim 10 m wind, all model runs starting from slightly different initial conditions on January 1, 1980 (Thoma et al., 2015a). For the hindcast simulations (Thoma et al., 2015b), the NCEPcfsr product was used to provide wind stress directly for the initialization run which, in turn, consisted of 3 ensemble members starting in 1980. These 3 ensemble members were branched into 18 ensemble members for the hindcasts themselves.

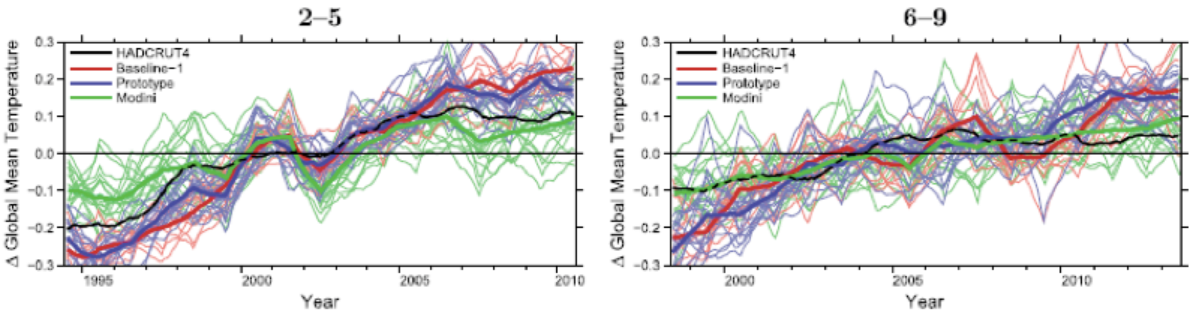

Figure 1. Time series (4 year running means) of global mean temperature anomalies for the hindcast years (left) 2-5 and right (6-9) for first forecast years from 1990 to 2006. Anomalies are estimated with respect to the respective mean of each individual graph. Green (red, blue) thick line indicates the ensemble mean result for MODINI (Baseline-1, Prototype). Thin lines show individual ensemble members. Black lines indicate 4 year running mean observations as reference according to HadCRUT4 median. Note that the value assigned to the abscissa corresponds to the centre of the hindcast period.

The above work has led to two recent publications:

Thoma, M., R. Gerdes, R.J. Greatbatch and H. Ding, 2015a: Partially coupled spin-up of the MPI-ESM: implementation and first results., Geosci. Model Dev. Discuss., 8, 51-68, doi:10.5194/gmd-8-51-2015.

Thoma, M., R.J. Greatbatch, C. Kadow and R. Gerdes, 2015b, Decadal hindcasts initialised using observed surface wind stress: Evaluation and Prediction out to 2024, Geophys. Res. Lett., 42 (15). pp. 6454-6461. DOI 10.1002/2015GL064833.